

Analyses of anomalous amplitudes of antipodal PKIIKP waves

WenShuang Wang¹, and XiaoDong Song^{1,2*}

¹School of Geodesy and Geomatics, Wuhan University, Wuhan 430079, China;

²Department of Geology, University of Illinois at Urbana-Champaign, 61820, USA

Abstract: Approaching the distance of 180°, seismic focusing greatly amplifies the normally weak PKIIKP phase (underside reflection from the inner core boundary). Anomalously strong amplitudes of the PKIIKP phase reported previously at near antipodal distances (at seismic station TAM in North Africa) have been interpreted to infer anomalous structure(s) of the inner core boundary (including a sharp drop of compressional wave speed in the bottommost outer core or a near-zero shear wave speed in the topmost inner core). However, our observations of 12 earthquakes located antipodal to TAM (including the previously cited four events) suggest, for several reasons, that the anomalous PKIIKP energy might be a seismic phase misidentification. The anomalous phase appeared at distances less than 179.6° but not at larger distances (~179.8°). The phase appears consistently from antipode to distances less than 160° and has horizontal slowness similar to the PKIKP phase (going straight through the inner core). Its travel times vary greatly and show a systematic difference between two groups of events at different distances. A simple point scatter provides a good match to the travel times and the systematic variation of the anomalous phase at most stations, suggesting that it could originate from scattering off strong heterogeneities in the mantle wedge above the subducting Tonga slab. The phase misidentification suggests that the previously proposed inner core boundary structure(s) based on the anomalous phase need to be re-evaluated.

Keywords: PKIIKP; PKIKP; antipodal; inner core; amplitude; scattering

Citation: Wang, W. S., and Song X. D. (2019). Analyses of anomalous amplitudes of antipodal PKIIKP waves. *Earth Planet. Phys.*, 3(3), 1–6. <http://doi.org/10.26464/epp2019023>

1. Introduction

PKIIKP wave, reflected from the underside of the inner core boundary, traverses the inner core from either the minor-arc or the major-arc direction at a near antipodal distance (Figure 1). The amplitude of PKIIKP will increase greatly as the distance increases from 178° to 180°, but it is still weaker than that of PKIKP (the wave going through the center of the Earth) for a standard Earth reference model. Thus, it is worth noting that [Butler and Tsuboi \(2010\)](#) (hereafter referred to as BT10) observed four anomalous PKIIKP amplitudes at distances of 179° to 180° from earthquakes in the Tonga subduction zone, recorded at station TAM (Tamanrasset, Algeria) of the GEOSCOPE seismic network ([Pardo et al., 2009](#)). They attribute the origin of this anomaly mainly to a sharp ~15% drop in V_p in the bottommost outer core.

Such a sharp drop of V_p in the bottommost outer core has been disputed ([Adam et al., 2018](#); [Souriau, 2015](#)). PKIIKP amplitudes at near antipodal distances are sensitive to the S velocity in the uppermost inner core, which undergo amplification of a factor of 4 or more as the shear modulus approaches zero ([Cormier et al., 2011](#); [Cormier, 2015](#)). Therefore, [Cormier \(2015\)](#) attributes the origin of the anomalous PKIIKP amplitudes [BT10] to a near-zero S velocity in the uppermost inner core.

When an inference is based on very few observations, such as the four anomalous PKIIKP amplitudes found by BT10, it is prudent to examine these observations carefully. In this study, besides the four earthquakes [BT10], we found other eight earthquakes with good signal-to-noise in a systematic search for earthquakes located nearly antipodal to station TAM. We analyzed the 12 events carefully and determined that the anomalous PKIIKPs identified by BT10 were likely a misidentification. The anomalous amplitudes might be from waves scattered near the sources. Thus, the proposed inner core structure that was based on the anomalous data needs to be re-evaluated.

2. Data

We first searched systematically, in the Incorporated Research Institutions for Seismology (IRIS) Data Management System, for earthquakes in the Tonga subduction zone that were located nearly antipodal (179°–180°) to TAM. We sought earthquakes of magnitude 5.3 or greater from January 1990 to April 2018 that had clear PKIKP signals. Besides the four anomalous events above, we found eight other events that met our requirements ([Table 1](#); [Figure 2](#)). Note that all the 12 events are shallow events. We didn't find any deep events that satisfy our criteria in the systematic search, even though the Tonga subduction zone is one of the most active deep subduction zones in the world. Because of the subduction zone geometry with dipping angles, all the deep events are at less than 179°, thus out of the antipode to TAM. We then searched all seismograms of PKP waves in the distance

Correspondence to: X. D. Song, xiao.d.song@gmail.com

Received 28 JAN 2019; Accepted 14 MAR 2019.

Accepted article online 15 APR 2019.

©2019 by Earth and Planetary Physics.

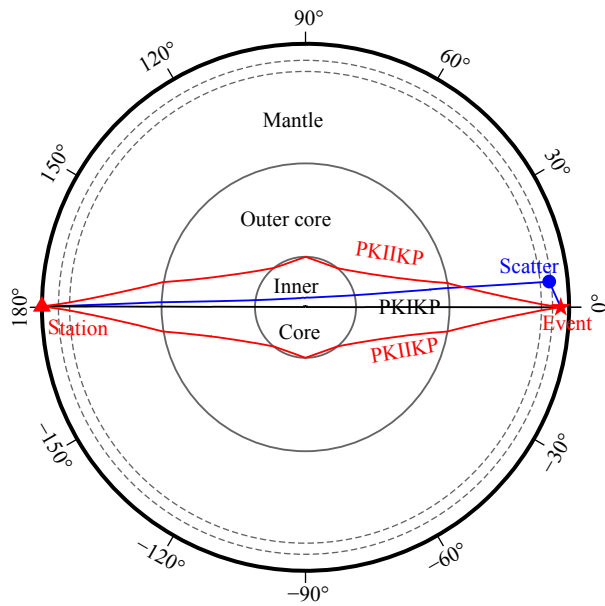


Figure 1. Ray paths of seismic phases passing through inner core, PKIKP (black), PKIIP (red), and scattered PKIIP (blue) waves.

ranges of 150° – 180° and mantle P waves at smaller distances for these events in order to study the characteristics of the antipodal phases. Except for TAM station, we didn't find any seismograms in 170° – 180° for these events. Figure 2 shows the locations of the 12 events and station TAM and some other stations relatively close to TAM. We used only the vertical components of broadband seismograms in this study.

Our preprocessing of data followed this sequence:

(1) The instrument response was deconvolved and the original broadband seismogram was converted to displacement. (2) Means and trends were removed; the sampling period was interpolated to 0.01 s to improve the accuracy of phase picks. (3) A band-pass Butterworth filter (0.1 to 2 Hz as in Figure 3) was ap-

plied. (4) Arrival times of PKIKP were picked by hand: as the PKIKP arrivals are clear in these seismograms, we simply selected the peak amplitude of the beginning part of the phase consistently for different stations. (5) We determined the PKIIP time window, using a 10-s time window centered on the theoretical arrival time of PKIIP (Figure 3a). The 10-s threshold was chosen to reduce the interference of the neighboring phase PKP-C_{diff} when picking the PKIIP phase (Attanayake et al., 2018). The peak amplitude near the beginning portion of the time window was selected as the determinant of PKIIP arrival time. We further used cross-correlation between two stations's data of the same event to examine the consistency of the phase picking and adjust the time pick if necessary. (6) The seismogram was normalized by the peak amplitude of PKIKP, to facilitate comparison of PKIIP amplitude relative to PKIKP.

3. Results and Discussion

In this section, we examine the seismograms in different ways, demonstrating that the anomalous PKIIP arrivals at TAM [BT10] are likely misidentified. We suggest that they might be scattered waves from strong heterogeneities above the subducting Tonga slab.

3.1 Seismograms at Station TAM

The 12 selected events were divided into three groups according to the event locations (Figure 2a) and epicentral distances and waveform similarities (Figure 3a) (see more discussion below). The events with anomalous PKIIP arrivals, including those previously identified by BT10, were divided into Groups A and B. Events in both of these groups exhibit a strong signal (hereafter referred to as the M phase) in the time window of PKIIP. This signal is not seen in events in Group C. Thus, it is reasonable to infer that the M phase is not from a shallow structure near station TAM.

We used an explosion source to calculate synthetic seismograms for the PREM model (Dziewonski and Anderson, 1981) using the

Table 1. Twelve earthquakes in this study*

Group	Date	Time (UTC)	Latitude (°)	Longitude (°)	Depth (km)	Mag (M _b)	Distance (°)
A	1993/01/04	20:41:12.4	-22.06	-174.81	43.9	5.9	179.21
A	1993/02/20	07:11:51.6	-22.00	-174.85	36.2	5.6	179.14
A	1997/10/19	15:53:39.1	-21.96	-174.89	35.0	5.6	179.08
A	2000/08/17	00:04:29.7	-22.02	-174.65	38.7	5.8	179.22
A	2004/04/24	07:44:09.5	-21.96	-174.72	4.3	5.7	179.14
A	2004/06/14	20:06:15.5	-22.19	-174.85	33.0	5.5	179.31
A	2010/02/13	02:34:29.4	-21.95	-174.75	16.4	6.0	179.13
B	1992/09/10	10:43:20.1	-22.60	-174.90	37.7	5.6	179.56
B	2001/09/15	15:04:39.0	-22.45	-174.92	43.7	5.9	179.47
B	2011/07/16	07:03:36.8	-22.48	-174.88	34.6	5.7	179.51
C	2011/04/22	17:14:52.7	-23.01	-174.45	34.5	5.5	179.78
C	2011/07/11	10:48:35.0	-22.82	-174.64	34.2	5.6	179.84

*The earthquake location is from the ISC bulletins. The distance is to station TAM. The four events highlighted in dark are the same as in BT10.

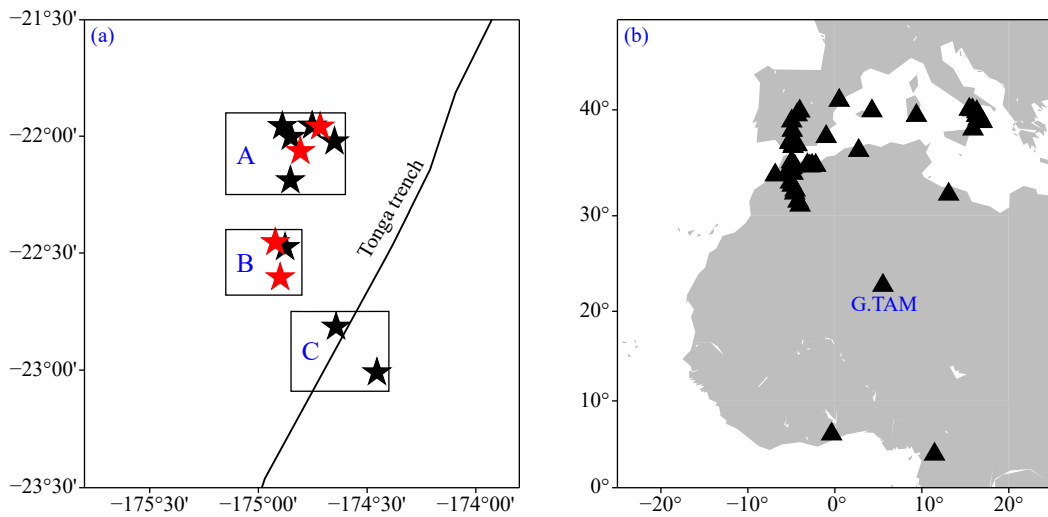


Figure 2. Maps of events (a) and station TAM and stations relatively close by (b) used in this study. The red stars in (a) indicate the anomalous PKIIKP events by BT10. The black line indicates the Tonga trench.

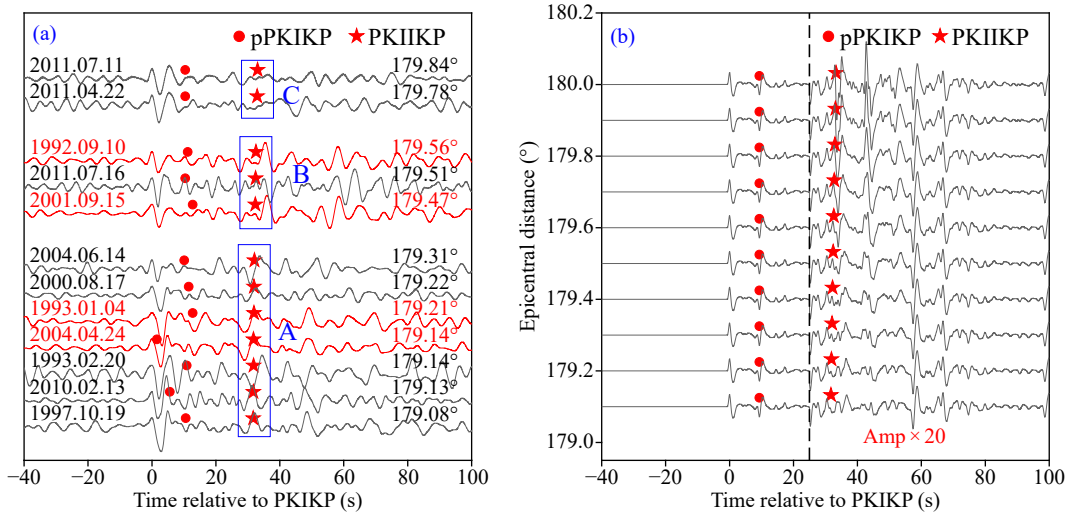


Figure 3. Observed seismograms at TAM (a) and synthetics near antipodal distances (b). The traces are aligned and normalized relative to the PKIKP phase (at zero time). Predicted times for PKIIKP and pPKIKP phases are marked with red star and dot derived for the PREM model (Dziewonski and Anderson, 1981). (a) Red traces indicate the four events with anomalous PKIIKP amplitudes from BT10. The traces are divided into three groups (A, B, C) (see labels in the plot). Rectangular window indicates the 10-s time window centered at the theoretical PKIIKP time for each group. The strong signals in the PKIIKP window in Groups A and B are referred to as the M phase in this study. (b) Synthetic seismograms calculated for DSM (Takeuchi et al., 1996) for an explosion source at 30-km depth. Waveforms after the vertical dashed line are amplified by a factor of 20.

DSM method (Takeuchi et al., 1993) (Figure 3b). The synthetics of BT10 show that the earthquake radiation pattern has a negligible effect on PKIIKP amplitudes (relative to PKIKP) for the four anomalous PKIIKP amplitudes and in a general case. Furthermore, there are different events recorded at stations with different azimuths. Thus, we used an explosion source to generate synthetics to examine the propagation effect from the reference model. The amplitudes of PKIIKP in the synthetics were amplified by a factor of 20 (Figure 3b), only by which the PKIIKP phase shows comparable amplitudes with the M phase. The average distance between Group A and Group B is only about 0.5° (Figure 2a), thus it is reasonable to infer that the M phase in these events originates from a

similar structure.

The amplitudes of the M phase were extremely strong. A sharp V_p drop of ~15% in the bottommost outer core [BT10] or a near-zero S velocity in the uppermost inner core (Cormier, 2015) could amplify the amplitude of PKIIKP, but the PKIIKP phase reaches the amplitudes of the M phase only at distances of 179.7° to 180° for these anomalous models. On the other hand, the distances for the 10 events in group A and B at station TAM are in the range 179° to 179.6° (Figure 3a), while the two events in group C are at larger distances (about 179.8°) but do not show strong M arrivals. Thus even considering reasonable location uncertainty, we infer that the anomalous M phase may not be PKIIKP.

3.2 Recorded Waveforms at Multiple Stations

Examining seismograms from other stations for the same events (commonly known as the record section of the events), we note similar waveforms and amplitudes (relative to the PKIKP phase) of the M phase at distances of 158° to 170° (Figure 4). This phenomenon exists in all the events in Groups A and B. We thus infer that the arrival in TAM previously identified as PKIIKP is likely the same as the M phase detected at other stations. The differential travel times between the M phase and PKIKP do not change significantly as the distance increases from 158° to 170° , suggesting the phase has a similar ray parameter (horizontal slowness) to that of PKIKP. Thus it is reasonable to infer that the M phase may not be PKIIKP.

3.3 Relative Travel Times of the M Phase

We calculated the residual of the differential travel time between the M phase and PKIKP by subtracting from it (Figure 5) the theoretical PKIIKP-PKIKP differential time (for PREM). The variation of the differential travel time residuals at TAM is large (almost 4 s) within 178.8° – 179.8° (Figure 5a). The difference is systematic by some 3 s at TAM and other stations from 160° to 180° between Group A events and Group B events (Figure 5b). The variation within each group is also large (up to 3 s within Group A and 1 s within Group B).

The distance to TAM between Group A and Group B events is only about 0.5° (Figure 2a), thus their ray paths and ray path directions through the inner core are rather similar. Hence, it is reasonable to infer that any inner core anisotropy (Song XD, 1997) will affect similarly the travel times to station TAM of PKIKP and PKIIKP for these events. Influence of mantle heterogeneity and source location uncertainty can be estimated to be less than 0.9 s on the differential PKIIKP-PKIKP times at TAM (Niu FL and Chen QF, 2008). The 0.9-s threshold is significantly smaller than the variation of the observed differential time residuals of the M phase at TAM

(Figure 5a) or at other stations (Figure 5b); thus it is reasonable to infer that the M phase may not be PKIIKP.

3.4 A Possible Origin of the Anomalous M Phase

We argue above that the anomalous energy at TAM and its association with similar energy at other stations at distances 160° to 180° (the M phase) might not be the PKIIKP phase. The three groups of events (A, B, C) were initially divided according to waveform characteristics (amplitudes and travel times) at TAM in the PKIIKP time window (Figure 3a). However, it turned out that these three groupings also cluster the events by location (Figure 2a) and sort them according to their epicentral distances (Figure 3a). This remarkable co-incidence seems to point to an origin near the earthquake sources for the M phase.

Here we infer that the energy perhaps originates from scatter(s) near the events. Zheng YC et al. (2007) reported a series of anomalous sub-horizontal reflectors in the mantle wedge above the subducting Tonga slab. The existence of these reflectors and their variability in scale and in strength suggest strong heterogeneities in the mantle wedge. The distance between Group A and Group B is small (only about 0.5°) (Figure 2a), but the difference of the observed M-PKIKP residuals between the two groups is large (Figure 5b). The residuals from events in Group B are consistently larger than those in Group A by about 3 s at distances from 160° to 180° . In addition, the M phase does not appear in 30° – 90° (Figure 4). We argue that the anomalous M phase does not come from reflections of the sub-horizontal reflectors. All the events in this study are shallow events (Table 1). Reflections from the sub-horizontal reflectors cannot explain the 3-s systematic difference of the M arrivals between Groups A and B or the lack of strong M energy in Group C. The variation of the M phase appears more related to the groups' horizontal location differences.

We thus speculate that the M phase originates from scattering off strong small-scale heterogeneities near the earthquakes. The

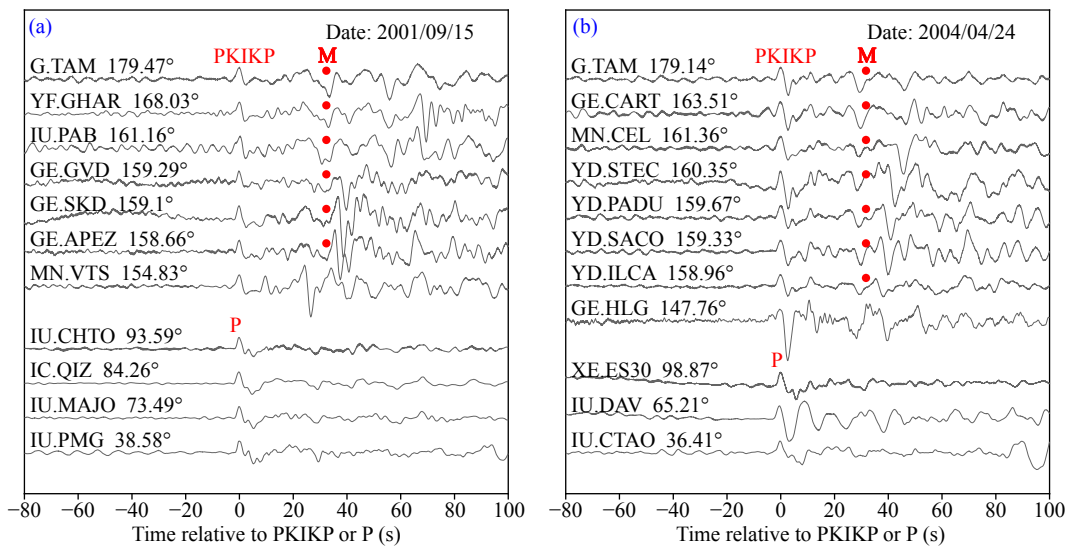


Figure 4. Record sections of two anomalous events, one from Group B (a) and the other from Group A (b). These two events are among the four events in BT10. Seismograms are aligned with PKIKP or P, and high-pass filtered at 100 s to match the previous observations as in BT10. The red dots indicate the M phase. The station name, network code, and epicentral distance are labeled.

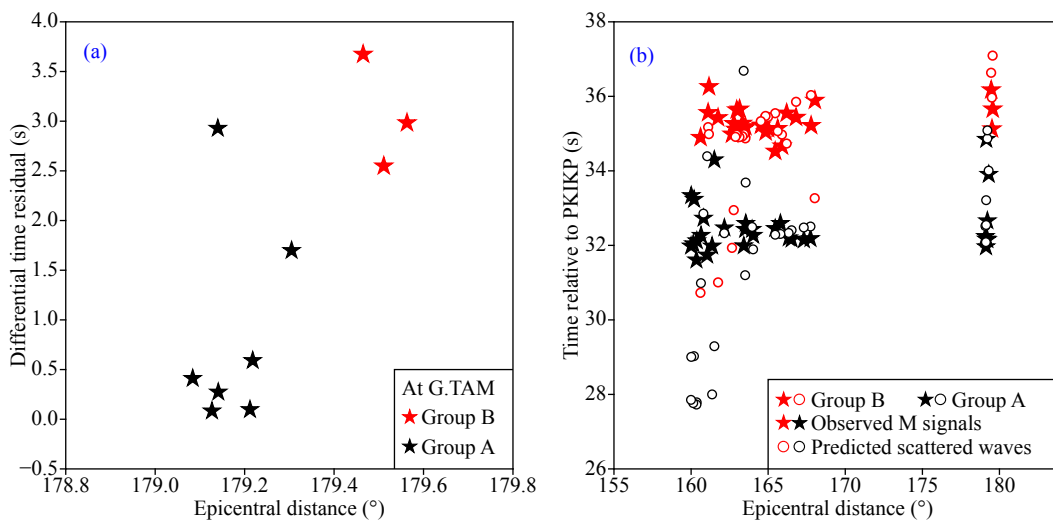


Figure 5. Relative times of the M phase. (a) Residuals of observed differential times M-PKIKP determined by subtracting predicted differential times PKIIPK-PKIKP at station TAM. Black and red stars indicate data from Groups A and B, respectively. (b) Differential travel times between the M phase and PKIKP. Black and red symbols are for Group A and red for Group B, respectively. Solid stars indicate observations and open circles indicate predictions for a point scatter at $(-18.7^\circ, -179.1^\circ, 450 \text{ km})$.

events in Groups A, B and C all show some apparent signals at station TAM after the PKIIPK time window (Figure 3a) and they are not as strong in Group C as in Groups A and B. The strong signals also appear after the M phase at other stations (Figure 4), which may be a further indication of scattering off small-scale heterogeneities near the source. Assuming a point scatter and calculating the travel times of scattered waves from the scatter, we found that a simple point scatter located at $(-18.7^\circ, -179.1^\circ, 450 \text{ km})$, which is in the vicinity of a strong reflector in Zheng YC et al. (2007), can match the observed data remarkably well. In particular, this point scatter yields the systematic difference in the M arrival times between Groups A and B at most stations (Figure 5b). It also produces strong variability in travel times of the scattering waves as in the M phase in either group. However, some observations of the M phase couldn't be matched (Figure 5b), which may indicate additional scatterer(s). Similarly, other scatters could account for strong arrivals after the PKIIPK window in Groups A and B, as well as less strong but apparent signals in Group C before and after the PKIIPK window (Figure 3a).

4. Conclusions

In this study, we examined anomalous PKIIPK amplitudes at station TAM first identified by BT10. We systematically searched for earthquakes recorded at station TAM at near antipodal distances. We found 12 events with clear PKIIPK phase, which we divided into three groups (A, B, C). The two events in non-anomalous Group C do not show clear arrivals in the PKIIPK window, while the 10 events in anomalous Groups A and B (which include the four events cited in BT10) show strong energy (called the M phase) in the time window. We conclude that the anomalous PKIIPK arrivals at TAM in previous studies were likely a misidentification. We present several lines of evidence as summarized in the following.

(1) Synthetics suggest that strong focusing occurs when the distance approaches 180° . However, the strong M phase appears at TAM at distances of 179° to 179.6° from events in Groups A and B,

but does not appear at the larger distances ($\sim 179.8^\circ$) of events in Group C.

(2) The M phase appears at other stations and has ray parameters not consistent with PKIIPK but instead similar to those of the PKIKP phase.

(3) The travel times of the M phase (relative to PKIKP) at TAM show large variation between Group A and Group B as well as within each group. The large variation is difficult to explain by an inner core structure.

(4) The travel time difference of the M phase between Groups A and B is systematic from 160° to 180° , unlikely to be caused by an inner core structure.

(5) The event groupings (A, B, C) show a remarkable co-incidence of location, waveform, travel time, and distance, pointing to an origin near the earthquake sources.

(6) Scattering near the earthquakes can produce energy at PKIIPK time window or other windows after PKIKP.

Instead of an inner core structure, we suggest that the more probable cause of anomalous arrivals in the PKIIPK time window at TAM might be scattering off strong heterogeneities in the mantle wedge above the subducting Tonga slab. A simple point scatter located at $(-18.7^\circ, -179.1^\circ, 450 \text{ km})$ near a strong reflector identified by Zheng YC et al. (2007) could generate scattering energy at the PKIIPK window and could explain the systematic difference in travel times of the M phase between the Groups A and B at most of the stations.

Acknowledgments

We thank two anonymous reviewers for constructive reviews. The seismic waveform data were obtained from the IRIS Data Management Center. The figures were prepared using Generic Mapping Tools (Wessel et al., 1998). The research was supported by Nation-

al Science Foundation of China (41774056) and the US National Science Foundation (EAR 1620595).

References

Adam, M. C., Ibourchène, A., and Romanowicz, B. (2018). Observation of core sensitive phases: constraints on the velocity and attenuation profile in the vicinity of the inner-core boundary. *Phys. Earth Planet. Inter.*, 275, 19–31. <https://doi.org/10.1016/j.pepi.2017.12.008>

Attanayake, J., Thomas, C., Cormier, V. F., Miller, M. S., and Koper, K. D. (2018). Irregular transition layer beneath the Earth's inner core boundary from observations of antipodal PKIKP and PKIKP waves. *Geochem. Geophys. Geosyst.*, 19(10), 3607–3622. <https://doi.org/10.1029/2018GC007562>

Butler, R., and Tsuboi, S. (2010). Antipodal seismic observations of temporal and global variation at Earth's inner-outer core boundary. *Geophys. Res. Lett.*, 37(L11), L11301. <https://doi.org/10.1029/2010GL042908>

Cormier, V. F., Attanayake, J., and He, K. (2011). Inner core freezing and melting: Constraints from seismic body waves. *Phys. Earth Planet. Inter.*, 188(3-4), 163–172. <https://doi.org/10.1016/j.pepi.2011.07.007>

Cormier, V. F. (2015). Detection of inner core solidification from observations of antipodal PKIKP. *Geophys. Res. Lett.*, 42(18), 7459–7466. <https://doi.org/10.1002/2015GL065367>

Dziewonski, A. M., and Anderson, D. L. (1981). Preliminary reference Earth model. *Phys. Earth Planet. Inter.*, 25(4), 297–356. [https://doi.org/10.1016/0031-9201\(81\)90046-7](https://doi.org/10.1016/0031-9201(81)90046-7)

Niu, F. L., and Chen, Q. F. (2008). Seismic evidence for distinct anisotropy in the innermost inner core. *Nat. Geosci.*, 1(10), 692–696. <https://doi.org/10.1038/ngeo314>

Pardo, C., Bonaime, S., Stutzmann, E., Maggi, A., and Group, G. (2009). New developments of the geoscope program. In *American Geophysical Union, Fall Meeting 2009*. Washington: AGU.

Song, X. D. (1997). Anisotropy of the Earth's inner core. *Rev. Geophys.*, 35(3), 297–313. <https://doi.org/10.1029/97RG01285>

Souriau, A. (2015). Presumption of large-scale heterogeneity at the top of the outer core basal layer. *Earth. Planet. Sci. Lett.*, 415, 175–182. <https://doi.org/10.1016/j.epsl.2015.01.024>

Takeuchi, N., Geller, R. J., and Cummins, P. R. (1996). Highly accurate P-SV complete synthetic seismograms using modified DSM operators. *Geophys. Res. Lett.*, 23(10), 1175–1178. <https://doi.org/10.1029/96GL00973>

Wessel, P., Smith, W. H. F., Scharroo, R., Luis, J., and Wobbe, F. (2013). Generic Mapping Tools: Improved version released. *Eos*, 94(45), 409–410. <https://doi.org/10.1029/2013EO450001>

Zheng, Y. C., Lay, T., Flanagan, M. P., and Williams, Q. (2007). Pervasive seismic wave reflectivity and metasomatism of the Tonga mantle wedge. *Science*, 316(5826), 855–859. <https://doi.org/10.1126/science.1138074>